Dust explosion development in a vessel-duct arrangement

Yann Gregoire, Christophe Proust, Emmanuel Leprette

Dust explosion development in a vessel-duct arrangement

Grégoire Y.[a], Proust C.[a,b], Leprette E.[a]

E-mail: *yann.gregoire@ineris.fr*

[a] INERIS, PHDS dpt, Parc Technologique ALATA, BP 2, 60550 Verneuil-en-Halatte, France
[b] UTC, TIMR laboratory (EA4297), rue du Dr Schweitzer, 60200 Compiègne, France

Abstract

In many practical situations, a flame may appear inside a vessel and start to propagate inside the connected pipes. It may be a very hazardous situation and several mitigation means were developed to stop the subsequent explosion escalation (chemical barriers, gate valves, flap valves, diverters). There is a need to better understand the development of the explosion in such a situation. Unpublished data are presented in the present paper using mainly the ISO 1 m3 vessel connected to ducts with an internal diameter varying between 100 mm and 440 mm (length between 0 and 10 m). Four very different dusts were used. In all situations a strong link is found between the vessel overpressure and the flame velocity along the duct. Moreover, all along the period during which the flame rushes down the pipe, the discharge of the vessel is severely impeded and this phenomenon is believed to explain the very significant incidence of even a relatively short portion of duct on the explosion overpressure inside the duct as claimed into the vent dimensioning standards.

Keywords: *dust explosions, vented explosions, flame propagation*

1. Introduction

Over the last decades, a significant number of experimental studies demonstrated that the dust explosion venting technique can be applied to a wide range of industrial situations and that it is possible to establish reasonable dimensioning rules to estimate the required vent areas. A number of guidelines or standards were developed to help the designers in France (AFNOR), in the USA (NFPA), in United Kingdom (BSI), in Germany (VDI). It was observed that the results provided by these methods differed significantly (Roux, 2000). In an effort to harmonize the practices and to cover more situations additional work was performed during the last ten years which resulted in upgraded versions of VDI3673, EN14491 and NFPA68 documents which tend to become international references. Nevertheless a number of important shortcomings of subsist and, among them, the influence of a duct attached on a vent. In the present paper additional results and interpretation is proposed about the propagation of explosion in a vessel-pipe arrangement and about the influence of "vent ducting" on the reduced explosion overpressure (P_{red}). Both the state of the art and the new results/interpretation are presented hereafter.

2. Guidelines and standards

Before 1980, only limited experimental evidence was available on the way the exhaust pipe connected to a vent could be accounted for. To our knowledge, the physical interpretation was still limited and little modeling was performed. In VDI 3673 (1979) (and in NFU54-540), the increase of P_{red} in the vented vessel due to the presence of the exhaust pipe was given graphically (Figure 1). For pipe longer than 3 m, P_{red} was at the least doubled, which is very large and the stepwise behavior of the correlation around a duct length of 3 m was difficult to understand and to accommodate for in practice. Apparently this graph was issued for a small set of data obtained by Bartknecht (1981).
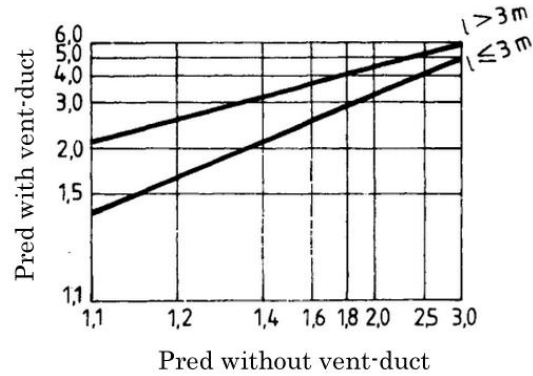

Figure 1: Effect of a vent-duct (of length l < 6 m) on the pressure in the vessel according to VDI 3673(1979)

Further work was performed in different institutes (section 3) which resulted in refined experimental correlations which were integrated at the turn of the century in the revised version of VDI 3673 (2002), NFPA68 (2002) and in the new born European standard EN 14491 (2002) (Table 1).

Table 1: 2002 models for the vessel pressure increase due to the addition of a vent duct

Equation		Source
$P'_{red,max} = P_{red,max} \times (1 + 17,3 \times (S \times V^{-0.753})^{1,6} \times l)$	(1)	VDI3673-2002
$P'_{red,max} = P_{red,max} \times (1 + 17,3 \times (S \times V^{-0.753})^{1,6} \times l/D)$	(2)	NFPA68-2002 & EN14491-2002

where:

- $P'_{red,max}$ is the maximum reduced explosion overpressure in the protected vessel with vent duct, in bar;
- $P_{red,max}$ is the maximum reduced explosion overpressure without vent duct, in bar;
- S is the vent area, in square-meters (m^2);
- V is the vessel volume, in cubic-meters (m^3);
- l is the length of vent duct, in meters (m).
- D is the duct hydraulic diameter (m)

Note that in Table 1, the $P'_{red,max}$ is a function of:

- the pipe length in VDI3673-2002,

- the ratio of the pipe length over its diameter in NFPA68 2002 and EN14491-2002.

The CEN norm also mentions an additional model for predicting the minimal duct length from which the P_{red} is modified. It is stated in the norm that the influence of the vent-duct becomes significant when the flame velocity in the duct reaches the sound celerity. The equation based on this statement in the norm is:

$$\frac{l_{lim}}{D} = 4.564 \cdot P_{red,abs}^{-0.37}$$ (3)

where D is the vent duct hydraulic diameter, and l_{lim} the limiting length above which a lengthening of the duct would have no effect on the P'_{red}. Note that a very similar equation exists in VD3673-2002, in which the pipe diameter is ignored (D=1). Equation (3) was established considering that the pressure increase in the vessel subsequent to the addition of a duct is due to a secondary explosion in the duct. In these documents (VDI3637, NFPA68 and EN14491, 2002), it is admitted that while the flame propagation in the duct remains subsonic the explosion discharge is not disturbed. Thus the l_{min} corresponds to the pipe length from which the flame reaches the sound velocity.

Siwek (2006) compared the results given by these formulas to experimental data obtained by Lunn (1988) and concluded that the VDI3673-2002 formula was more accurate for volumes smaller than 30 m³. Note that the formula suggested in VDI3673-2002 is now also used in the last issue of EN14491 (2012) (more exactly, this formula is used since the 2006 revision of the EN14491) while in the 2007 update of the NFPA68, a new and very different formula is given (Ural, 2005), integrating resistance coefficients of the vent ducts and the effect of some of their singularities, such as the effect of elbows or obstructions in the calculation of the needed vent area. At the time of writing of the present paper, the authors lack of fundamental information on the description of the models used in NFPA68. Thus the detailed comparison of these models with INERIS results will be the object of a further revision of this paper.

3. Available experimental data

A few experimental results concerning studies conducted before 1987 that were gathered by Siwek (1989) are presented in Table 2 with only very limited experimental details (nature of the vent cover ?, geometry of the duct ?…)

Table 2: Experimental results gathered by Siwek (1989)

Source	Vessel	Vent duct	P_{red} without vent-duct	P_{red} with vent-duct
Bartnecht, 1987	7 m³	$D = 500$ mm, $l = 5$ m	0.30 bar	3.00 bar
Hattwig, 1978	30 m³	$D = 1200$ mm, $l = 3$ m	1.20bar	1.90 bar

Experiments were also done in France in the 70's with vessels of 1 m³, 10 m³ and 100 m³ (Pineau, 1983). The main results are presented in Table 3 (vents openings of same cross section as the duct, no vent covers, straight pipes).

Table 3: Experimental results of Pineau (1983)

Dust	Vessel	Vent duct	P_{red} without vent-duct	P_{red} with vent-duct
Wheat flour	1 m³	$D = 50$ mm, $l = 10$ m	5.90 bar	7.20 bar
Wood flour	1 m³	$D = 50$ mm, $l = 10$ m	6.00 bar	8.10 bar

Dust	Vessel	Vent duct	P_{red} without vent-duct	P_{red} with vent-duct
Wheat flour	10 m³	$D = 700$ mm, $l = 3$ m	0.65 bar	0.75 bar
Wheat flour	10 m3	$D = 700$ mm, $l = 6$ m	0.65 bar	0.95 bar
Wheat flour	10 m³	$D = 700$ mm, $l = 9$ m	0.65 bar	1.15 bar
Milk powder	100 m³	$D = 900$ mm, $l = 3$ m	0.22 bar	0.22 bar

HSL teams also conducted several well documented tests (Lunn, 1988, 1998). A 18.5 m³ vessel was connected to pipes of lengths ranging between 1 and 11m, of diameters 0.5 to 1.1 m. The dust was injected through 3 "pressure vessels with peper pot nozzles" containing the same amount of dust. Lunn (1988) adjusted the dispersion pressure and ignition delay for each of the tested dusts in a view to obtain the same *Kst* values as in the reference 20 *l* sphere tests. Resulsts of the calibration tests performed by Lunn (1988) are summarized in Table 4.

Table 4: Dust properties Lunn's test (1988)

Dust	Injection pressure (bar)	Ignition delay (ms)	Concentration (kg/m3)	Kst (bar.m/s)	Pmax (bar)
Charcoal	20	760	0.5	144	8.5
Aspirin	30	540	1.0	254	8.3
Toner	20	760	0.25	236	8.8

Test results obtained by Lunn are listed in Table 5 and Table 6(vents of same cross section as the duct, no vent covers, straight ducts).

Table 5: Experimental results of Lunn (1988)

Dust	Vessel	Vent duct	P_{red} without vent-duct	P_{red} with vent-duct
Charcoal	18,5 m³	$D = 1100$ mm, $l = 1$ m	0.12 bar	0.10 bar
Charcoal	18,5 m³	$D = 1100$ mm, $l = 6$ m	0.12 bar	0.20 bar
Charcoal	18,5 m³	$D = 1100$ mm, $l = 11$ m	0.12 bar	1.00 bar
Charcoal	18,5 m³	$D = 700$ mm, $l = 1$ m	0.80 bar	0.55 bar
Charcoal	18,5 m³	$D = 700$ mm, $l = 6$ m	0.80 bar	1.40 bar
Charcoal	18,5 m³	$D = 700$ mm, $l = 11$ m	0.80 bar	1.40 bar
Charcoal	18,5 m³	$D = 500$ mm, $l = 1$ m	1.55 bar	1.35 bar
Charcoal	18,5 m³	$D = 500$ mm, $l = 6$ m	1.55 bar	1.40 bar
Charcoal	18,5 m³	$D = 500$ mm, $l = 11$ m	1.55 bar	3.00 bar
Charcoal	18,5 m³	$D = 900$ mm, $l = 1$ m	0.25 bar	0.15 bar
Charcoal	18,5 m³	$D = 900$ mm, $l = 6$ m	0.25 bar	0.30 bar
Charcoal	18,5 m³	$D = 900$ mm, $l = 11$ m	0.25 bar	1.03 bar

Table 6: Experimental results of Lunn (1988)

Dust	Vessel	Vent duct	P_{red} without vent-duct	P_{red} with vent-duct
Aspirin	18,5 m³	$D = 1100$ mm, $l = 6$ m	0.60 bar	1.45 bar

Dust	Vessel	Vent duct	P_{red} without vent-duct	P_{red} with vent-duct
Aspirin	18,5 m^3	$D = 1100$ mm, $l = 11$ m	0.60 bar	1.55 bar
Aspirin	18,5 m^3	$D = 900$ mm, $l = 1$ m	1.10 bar	1.40 bar
Aspirin	18,5 m^3	$D = 900$ mm, $l = 6$ m	1.10 bar	1.80 bar
Aspirin	18,5 m^3	$D = 900$ mm, $l = 11$ m	1.10 bar	2.97 bar
Aspirin	18,5 m^3	$D = 700$ mm, $l = 1$ m	1.10 bar	1.40 bar
Aspirin	18,5 m^3	$D = 700$ mm, $l = 6$ m	1.10 bar	1.80 bar
Aspirin	18,5 m^3	$D = 700$ mm, $l = 11$ m	1.10 bar	2.97 bar
Toner	18,5 m^3	$D = 900$ mm, $l = 1$ m	1.05 bar	1.20 bar
Toner	18,5 m^3	$D = 900$ mm, $l = 6$ m	1.05 bar	2.30 bar
Toner	18,5 m^3	$D = 900$ mm, $l = 11$ m	1.05 bar	2.60 bar

These data globally confirm that the addition of an exhaust pipe increases P_{red} but to a lesser extent that suggested by figure 1. Furthermore, P_{red} and l do not seems to be the only relevant parameters. A discussion about the comparison with the formulae given in table 1 is postponed to a forthcoming section of this paper but it is interesting to notice that Lunn observed in a few instances a decrease of P_{red} when adding only a short piece of pipe (1 m). This feature is not accounted for by the CEN models. Simple head loss estimations may shed light on this phenomenon: a gas flow passing through an orifice will be altered, depending on the shape of the orifice. A thin orifice has a typical coefficient of discharge of 0.62, while that of an orifice followed by a short piece of pipe is 0.82 (see Figure 2).


Figure 2: Typical discharge coefficient for various types of orifices (Bonnet, 2006)

4. Novel experimental data

The ISO 1 m^3 vessel (ISO 6184/4) with the standard dust dispersion system and ignition procedure was used; it was connected to straight pipes of variable diameter (105, 250 and 400 mm) and variable length (0, 3, 7 and 10 m). Four chemically very different powders were used (lignite, rhodine, toner, and corn starch). The ignition point was located at the back of the chamber opposite from the pipe entrance, in a view to favor the development of the explosions and reach higher pressures.

The following measurements were done (see Figure 3):

- pressures (piezoresistive Kistler 4043A10) in the vessel and at the junction with the duct.
- flame position (photodiodes) in the vessel (2) and along the duct (every 2.5 m on average), including one at the junction with the chamber.
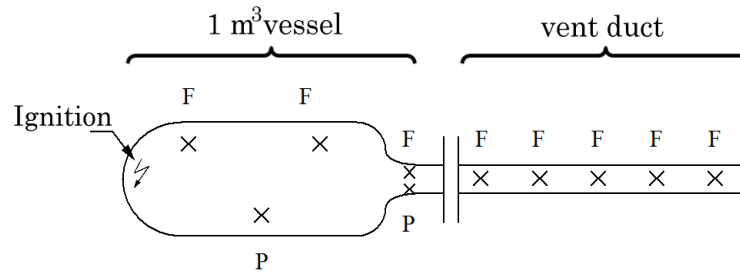

Figure 3: Scheme of the 1 m3 vessel with the attached vent duct. P= pressure sensor, F= flame detector

A picture of the 1 m^3 vessel is presented in Figure 4:

Figure 4 Picture of INERIS 1 m3 vessel (ISO 6184/4)

The explosion properties of the dusts were measured (Table 7) with the ISO 6184/4 1 m^3 vessel using the standard procedure (central ignition, closed vessel).

Table 7: Combustible dusts selected for the vent duct tests

Dust	lignite	rhodine	cornstarch	toner
Kst (bar.m/s)	135	160	110	120
P$_{max}$ (bar)	7,3	8,2	7,7	8,3
Concentration (kg/m^3)	750	1250	1250	500

For each dust and vent size, the concentration giving the highest pressure level in the vessel-duct arrangement was firstly determined with the longest vent duct (10 m). The subsequent

tests were performed keeping this concentration constant with shorter and shorter vent ducts (7, 3, and 0 m). About 50 different configurations were tested and the main results are presented in table 7.

Table 8: Experimental results obtained by Roux and Proust (2003)

Cornstarch						**Toner**				
l (m)	*D* (m)	*Pred* (bar)	*P'red* (bar)	*Vfmax* (m/s)		*l* (m)	*D* (m)	*Pred* (bar)	*P'red* (bar)	*Vfmax* (m/s)
10	0.25	0.52	3.3	500		10	0.25	1	4	625
7	0.25	0.52	3	350		7	0.25	1	3.22	585
3	0.25	0.52	1.9			3	0.25	1	3	625
10	0.105	5.8	5.85	500		10	0.105	5.2	5.5	625
7	0.105	5.8	5.96	435		7	0.105	5.2	5.6	875
3	0.105	5.8	6	415		3	0.105	5.2	5.43	625
10	0.4	0.18	1.92	360		10	0.4	0.29	2.4	360
7	0.4	0.18	1.9	350		7	0.4	0.29	2.4	350
3	0.4	0.18	1.2	250		3	0.4	0.29	1.35	335

Rhodine						**Lignite**				
l (m)	*D* (m)	*Pred* (bar)	*P'red* (bar)	*Vfmax* (m/s)		*l* (m)	*D* (m)	*Pred* (bar)	*P'red* (bar)	*Vfmax* (m/s)
10	0.25	1.75	4.4	625		10	0.25	0.4	2.8	500
7	0.25	1.75	4.1	435		7	0.25	0.4	2.6	390
3	0.25	1.75	3.1	310		3	0.25	0.4	1.7	310
10	0.105	5.4	6.3	625		10	0.105	4.86	5.6	625
7	0.105	5.4	6.3			7	0.105	4.86	5.5	435
3	0.105	5.4	6.4	625		3	0.105	4.86	5.7	310
10	0.4	0.54	2.32	500		10	0.4	0.19	1.55	335
7	0.4	0.54	2.32	520		7	0.4	0.19	1.7	370
3	0.4	0.54	1.7	285		3	0.4	0.19	0.79	235

5. Discussion

5.1 Flame propagation down the pipe

It is observed that the dust concentration for which P_{red} is maximal is on the order of 750 to 1000 g/m^3, for all the tested dusts. This range is comparable to those producing the most severe explosions in closed vessels (Kst measurements) Furthermore, the pressure signal measured in the vent duct is homothetic to that measured in the vessel but systematically of smaller amplitude. These two points suggest that, in the present configurations, the influence of the duct is mostly a mechanical resistance to the discharge and that the flame transmission through the pipe does not add much to the explosion[1]

In all of the tested configurations, the flames propagated all along the duct. The measured flame velocities were compared to the pressure in the vessel (Figure 5).

---

[1] An accelerating flame would change the shape of the signal or would even increase the pressure level in the duct as compared to that inside the vessel (Bouhard et al., 1990)
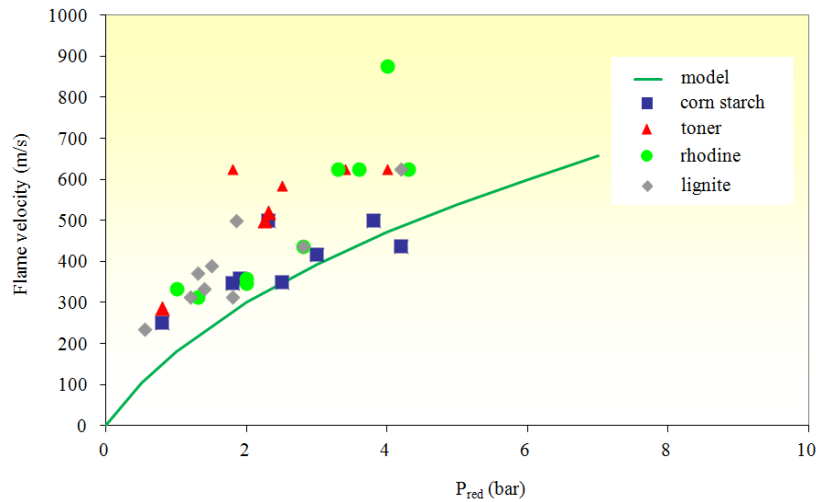
Figure 5: Flame velocity in the duct as a function of the reduced overpressure in the vessel

Despite the relatively poor accuracy of the velocity measurements ($\pm$ 50 – 100 m/s), a trend is seen showing that the flame velocity increases with the reduced pressure in the vessel. This correlation resembles closely that of the theoretical model giving the maximum flow velocity down the pipe pushed by the difference of pressure between the reservoir and the surrounding atmosphere[2]. Note that within the theoretical estimation, it is assumed that the flow velocity inside the pipe before the flame enters the duct is zero which is clearly not the case. Taking this into account, the agreement with the experiments is reasonable.

This observation confirms that the flame rushing down the pipe is "following" rather passively the flow field imposed by the difference of pressure between the reservoir and the surrounding atmosphere. The pipe would then mostly generate an airflow blockage leading to a pressure increase in the vessel. Similar conclusions were found by Lunn (1988) and Pineau (1983), who thought that this airflow blockage resulted from ''classical'' head losses due to friction at the wall. This point is discussed later (section 6).

5.2 *Reduced explosion overpressure (in the vessel)*

To compare with the data presented in section 3, two reduced pressures are listed in Table 8 (P'_{red} measured with a duct and P_{red} without). Clearly the effect of the vent-duct strongly depends on the pipe geometry and not only on the length of the pipe. For instance with cornstarch and a 10 m long-0.105 m diameter pipe $P_{red} \approx P'_{red}$, whereas with a 10 m long-0.4 m diameter pipe $P_{red} \approx 10$ x P'_{red}.

On Figure 6, a typical evolution of P_{red} with the increase of the pipe length is shown (rhodine dust, 400 mm ID pipe).

---

[2] This is the material velocity of a shock wave in which the pressure difference is the atmospheric pressure downstream and the pressure in the reservoir upstream (Kinney & Graham, 1985)
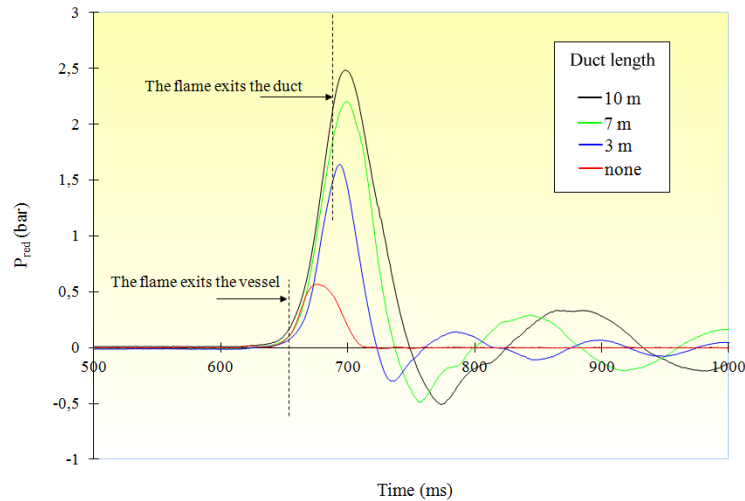
Figure 6: Reduced pressures in the vessel for an air-rhodine dust mixture (750g/m3) and a 400 mm diameter duct

In this example, the slopes of the pressure rises are all similar. This confirms that the combustion into the pipe does increase the dynamics (severity) of the explosion. This is coherent with the observation of the flame velocities. Slightly different results were obtained with toner dust (Figure 7).
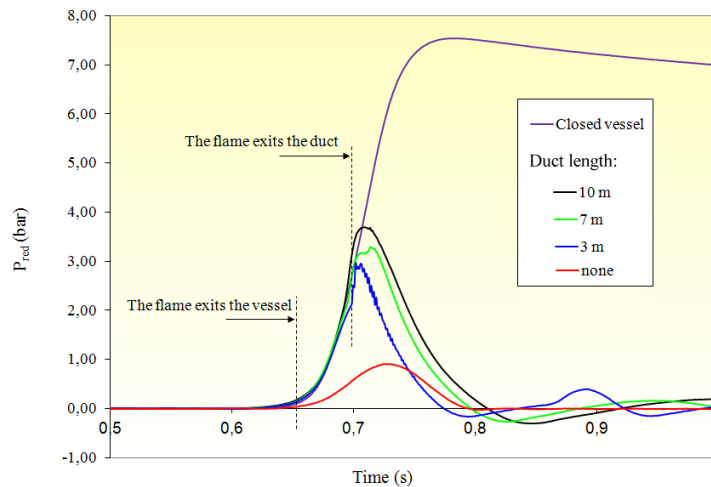

Figure 7: Reduced overpressures in the vessel for an air-toner dust mixture (500g/m3) and a 250 mm diameter duct

A slight modification of the slope of the pressure rise profile is observed around 0.7 s, between the closed vessel test and those with a vent-duct. This might be the consequence of some flame (self-)acceleration in the duct which was nevertheless not clearly identified by the photodiode arrangement, suggesting this extra phenomenon remained of limited extension. It is important to realize that, even in this case, the slope of the pressure rise is close to that obtained in the closed vessel, until the moment the flame reaches the end of the pipe. Again this point will be discussed further in section 6.

5.3 Effect of a singularity

In this paragraph, the term "singularity" refers to directional changes of the flow in the vent-duct (bend) and variations of its section (enlargement). Lunn (1988) investigated the influence of a bend located close to the exit of the duct. In some configurations a significant increase of P_{red} was observed (Figure 8) which cannot be simply correlated to the increase of flame path.
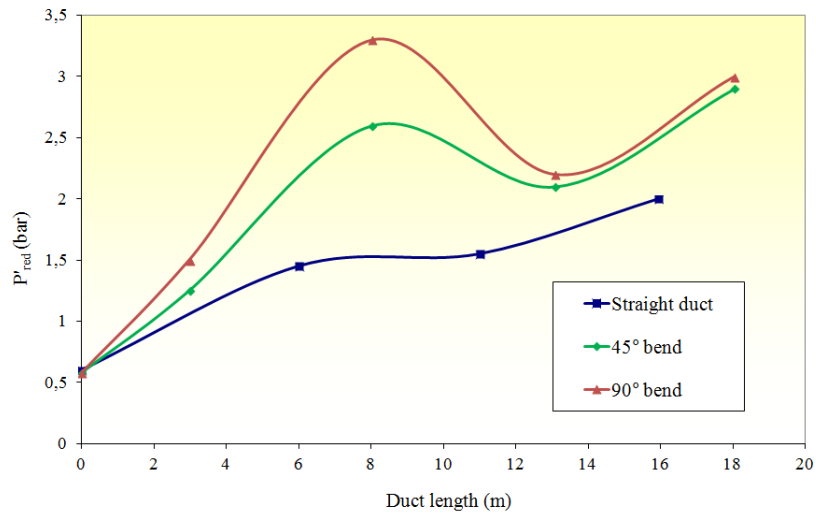

Figure 8 Pressure in a 18,5 m3 vessel for vent-ducts of same section but with a bend located at 1 m from the exhaust of the pipe (tests performed with aspirin, Kst = 200 bar.m/s)

Lunn also studied the influence of an enlargement of the pipe diameter immediately downstream the vent. Unexpectedly, the use of a pipe diameter much larger than the vent size does not reduce (at all) the increase of P_{red}.
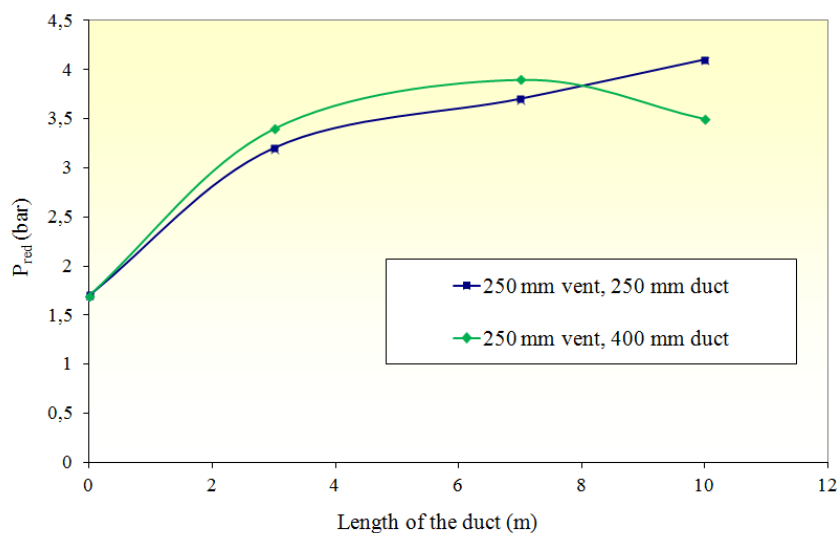

Figure 9 Effect of an increase of the duct section in comparison to that of the vent, on the reduced pressure in the vessel (rhodine, Kst = 160 bar.m/s)

Again this important finding is considered in the interpretation exercise below.

6. Interpretation

6.1 Phenomelogy.

Experimental results suggest that the pipe mostly generates an airflow blockage, which leads to the pressure increase in the vessel. The present section aims to shed light on the mechanisms that could be responsible for such blockage. The passing of the burnt gas flow in a duct will induce additional head losses. For this reason it seem logical to verify whether the head losses can be responsible for the observed gaps between P'_{red} and P_{red} or not.

To estimate the head losses in a pipe, the following correlations can be used[3] :

- Head losses in a straight portion of pipe:

$$\Delta P_{straight\_pipe} = \lambda_D \cdot \frac{l}{D} \cdot \rho \cdot \frac{U^2}{2} \tag{4}$$

where U is the flow velocity in the pipe, ρ its specific mass and λ_D the Darcy friction factor (typically 0.02)

- Head losses at a bend:

$$\Delta P_{bend} = 0.2 \cdot \rho \cdot \frac{U^2}{2} \tag{5}$$

with a radius of curvature of 2 and an angle between 45 and 90°

- Head losses for an enlargement after the vent:

$$\Delta P_{enl\arg ment} = \left(1 - \left(\frac{D_{vent}}{D}\right)^2\right) \cdot \rho \cdot \frac{U^2}{2} \tag{6}$$

U is the velocity at the vent (as if the pipe were of the same cross section than the vent of diameter D_{vent}).

U is related to P_{red} and is given in Figure 5. The specific mass of the air flow is taken at $P_{red}/2$ and ambient temperature to consider average values over the time of explosion. Applying these expressions to the situation of Figure 6 gives a typical gap between P'_{red} and P_{red} on the order of 0.6 bar for the 10 m long pipe well below the experimental result (2 bar). Since the head losses are proportional to l, the relative gap is even larger for shorter pipe length. Similarly, it is admitted (from the data of Figure 5) that flow velocity at the bend location (Figure 8) was about 350 m/s and P_{red} about 2 bar then the extra head losses would have been about 0.3 bar, much less than observed. Also, taking into account of the head losses would not permit to explain the shape of the curve. About, the pipe enlargement effect (Figure 9), since the vent areas are the same in both sets of experiments and since P_{red} are equal for the same duct length the mass flowrates should be the same. Rewriting the first and last equation above using the mass flowrates gives finally:

---

[3] Correlations for incompressible flows were used but are good enough to obtain orders of magnitude if average pressures are used.

$$\frac{\Delta P_{enl\arg ment}}{\Delta P_{straight\_pipe}} = \frac{\left(1-\left(\frac{D_{vent}}{D}\right)^2\right)+\lambda_D \cdot \frac{l}{D} \cdot \left(\frac{D_{vent}}{D}\right)^2}{\lambda_D \cdot \frac{l}{D_{vent}}} \tag{7}$$

It can be calculated that, in the experimental conditions of Figure 9, the ratio should by about 2 for 2 m long pipes and tends towards $(D_{vent}/D)^3$ (0.25) for very long pipes (this is only theoretical since P_{red} is limited to 5-7 bar).

Consequently, it is obvious that the head losses cannot explain satisfactorily the experimental trends and orders of magnitudes and an alternative mechanism needs to be looked for.

Although a complete description of the phenomenology remains out of hand, it seems possible to propose the main lines. It was observed first that the flame dynamics in the pipe obeys the shock wave theory, or, to be more accurate, behaves like an interface advected by the flow created by the "shock" wave[4]. Friction losses have little to do with this. Second, it is important to realize that this "interface" consumes the reactants producing expanding burnt products which counteract the discharge from the vessel. To some extent, the combustion occurring inside the pipe during the advection of the flame front may act as a "plug" refraining the discharge of the vessel. This conclusion is supported by some of the experimental observation telling that "the slope of the pressure rise is close to that obtained in the closed vessel, until the moment the flame reaches the end of the pipe". For the moment, it is hard to say more about the combustion regime in the pipe and especially how it is affected by the local flow (turbulence, flame curvature…).

Then the effect of a vent duct would be to delay the pressure unloading by a sort of "plug" effect. Some equations may be used to describe this. The data from Figure 5 (supported by the "shock" wave theory) suggest the following relationship between the flame velocity (U_{flame}) and P_{red}:

$$U_{flame} = k1 \cdot \sqrt{P_{red}} \tag{8}$$

with $k1$ a scalar on the order of 0,5 in SI units. Note that this model tends to underestimate the flame velocity for a given P_{red} (Figure 5). Thus a maximal transit delay time τ_c of the flame along a duct of length l can be defined:

$$\tau_c = \frac{l}{U_{flame}} \tag{9}$$

All along this period of time, the vessel pressure increases as if there were no vent, following a slope given by (Lewis and Von Elbe, 1987):

$$\frac{dP_{red}}{dt} = \gamma \cdot \frac{P_{red,abs} \cdot Q^+}{V} \tag{10}$$

Where $P_{red,abs}$ is the absolute pressure in the vessel, V its volume and Q^+ is the increase of volume induced by the combustion. γ is the specific heats ratio of the explosive cloud (generally $\gamma = 1,4$).

---

[4] In some handbooks, the shock wave is seen as the final (stable form) of an acceleration waves. This is exactly the effect the vessels produces inside the pipe while P_{red} increases.

It is recalled that when the vent (section S) is used without any exhaust pipe, the reduced explosion overpressure is reached when Q^+ equal the discharge flow rate Q^- so that (roughly, based on Bernoulli's theorem)

$$Q^+ = Q^- = k2 \cdot S \cdot P_{red}^{0,5} \tag{11}$$

where $k2$ is a scalar on the order of 1 in SI units.

Since P_{red} is reached as soon as the flame reaches the surrounding atmosphere, the incidence of the delayed exit of the flame due to the vent duct can approximately be described by:

$$P'_{red} = P_{red} + \frac{dP_{red}}{dt} \cdot \tau_c \tag{12}$$

Combining equations (8), (9), (10) and (11), equation (12) can be rewritten:

$$P'_{red} = P_{red} + \gamma \cdot P_{red,abs} \cdot S \cdot \frac{k2 \cdot l}{k1 \cdot V} \tag{13}$$

An experimental verification is proposed using the available results. A reasonable agreement is found both about the trends and in orders of magnitude indicating the physical interpretation might be on the right tracks.
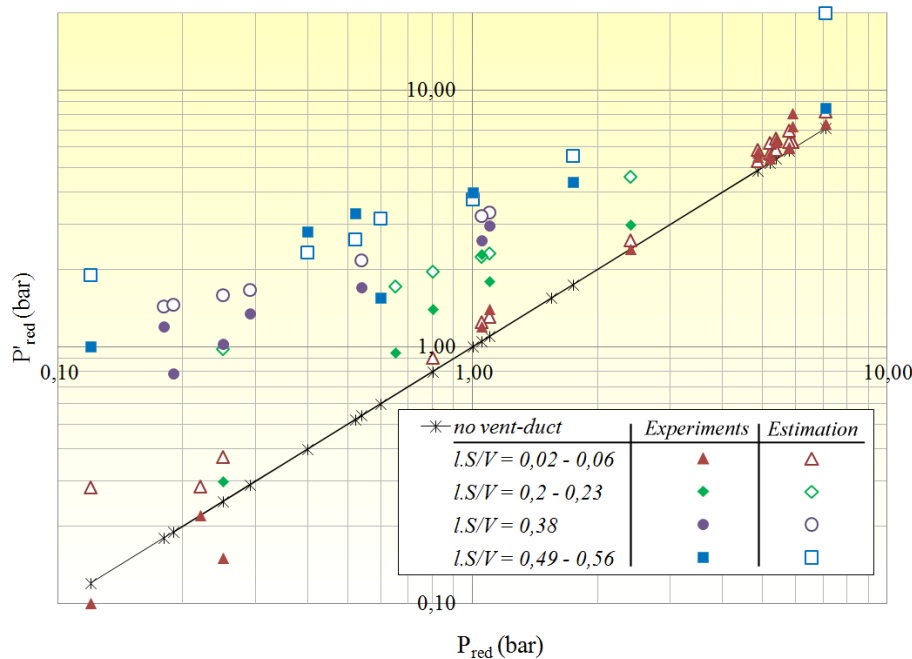

Figure 10 Evolution of P'red as function of Pred for different ranges of l.S/V values from all of the available data (Pineau (1983), Lunn(1988), Siwek(1989), INERIS)(Tables 2, 3, 5, 6 and 8)

This equation (13) would need to be improved to consider the compressibility of the flow and its possible supersonic behavior in some cases. However satisfying preliminary results are achieved: for a given P_{red}, a reasonable agreement between the P'_{red} measured experimentally and its value estimated equation (13) is found. Most of all, the trends seems nicely reproduced suggesting the physics was captured.

6.2   Correlations from the European standards

In the 2002 versions of EN14491, equation (2) was selected. But in the current version (2012) of the same document, equation (1) was, in which D was dropped. If the theoretical model (13) is slightly modified using $S.l/V \approx (S/V^{2/3})^{3/2}.l/D$ then:

$$\frac{P'_{red}}{P_{red}} = 1 + \gamma \frac{P_{red,abs}}{P_{red}} \cdot \frac{k2}{k1} \cdot \left(\frac{S}{V^{2/3}}\right)^{3/2} \cdot \frac{l}{D} \tag{14}$$

In many practical situations, P_{red} would be larger than 0,2 so that the term $\gamma \frac{P_{red,abs}}{P_{red}} \cdot \frac{k2}{k1}$ would be below or equal to 17. On this respect, this last equation would be closer to the formula of the EN14491-2002 standard. Nonetheless, it is clear that this coefficient is not a constant and it is worthwhile comparing the experimental data with all these equations.
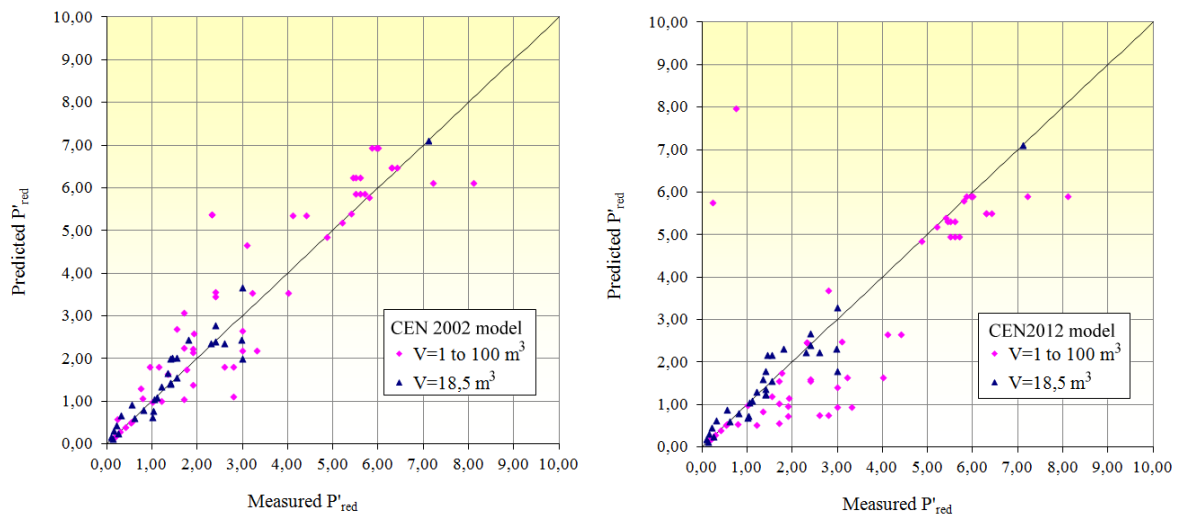

Figure 11 Comparison of the measured and calculated P'red between the experimental data and the predictions of the CEN formulas presented in equations (1) and (2) for the available data.

From the present experimental dataset, it can be estimated that the standards experimental deviation is ±30%. The CEN2002 correlation seems better that the CEN2012 version especially considering the fact that a significant number of situations may be severely underestimated. As most of these results were obtained on vessels smaller than 30 m³ (at the exception of Hattwig's test in a 30 m³ vessel and Pinneau's test in a 100 m3 vessel), this observation is consistent with the work of Siwek (2006) who concluded that the VDI3673-2002 formula was more accurate for volumes smaller than 30 m³. With both formula however, there is a significant risk that the scaling up would lead to incorrect results if it is admitted that equation (14) incorporates the physics.

The predictions obtained with equation (14) are compared to the same experimental dataset setting $k1$ and $k2$ at their theoretical values (0,5 and 1). Despite the wide spread of the experimental data is larger, more conservative results are obtained with this model, which is better in terms of industrial safety.
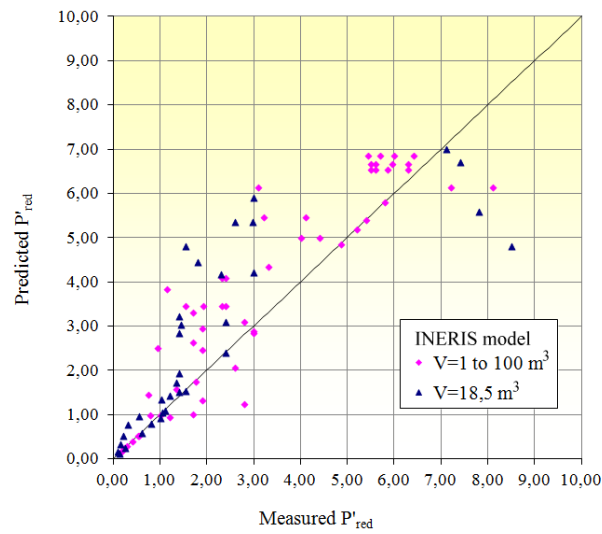
Figure 12 Comparison of the measured and calculated P'red between the experimental data and the predictions of the INERIS theoretical model presented in equation (13) for all of the available data (duct lengths inferior to 10 m and ST1 class dusts)

About this limiting length, l_{min}, below which the duct have no effect on P_{red}, the results obtained with the formula (3) are compared (Figure 13) with the present experimental dataset from Table 3 and Tables 5-6.
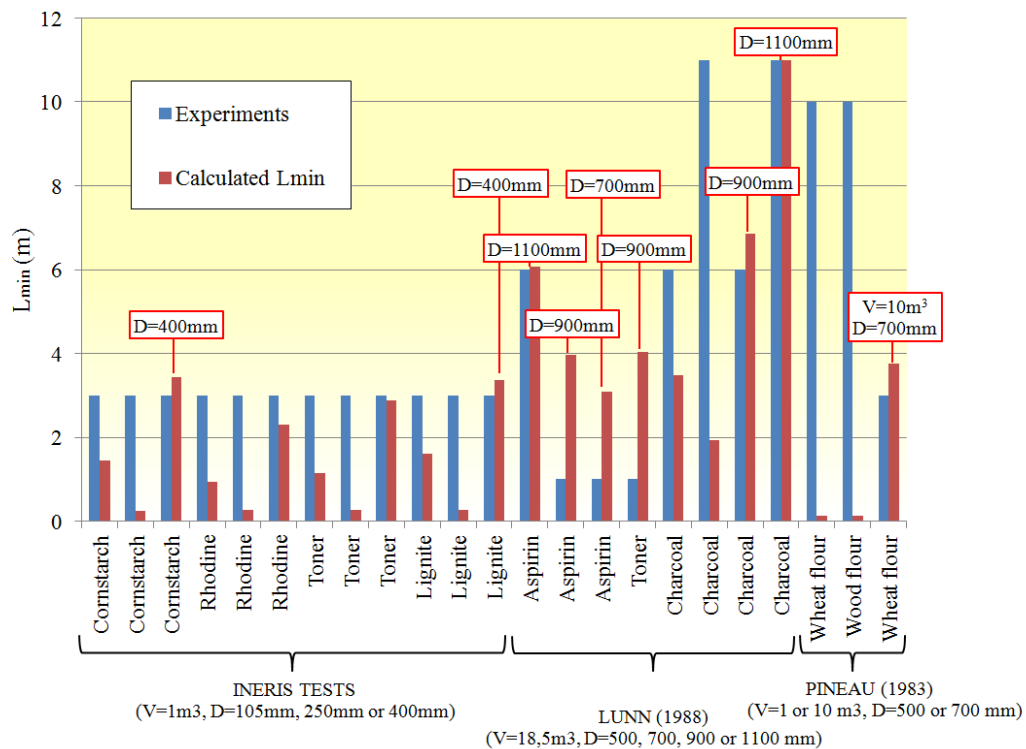

Figure 13 Comparison of the measured and calculated llim between the experimental data and the predictions of the CEN formula (3), for all of the available data. Data with a flag correspond to the cases in which the P'red is underestimated.

In Figure 12, in the experimental case, l_{min} designates the minimal length of the vent duct from which an increase of P_{red} to P'_{red} is noticed. As such the accuracy of the measurement is limited to the configuration tested, thus the experimental l_{min} is only majoring the real value and is expected to be longer or equal to the one calculated. When the calculation predicts a l_{min} longer than the experimental result, the model neglects the effect of the vent duct, which seems to be the case when:

- the explosion occurs in a larger enclosure (by comparison of Lunn and Pineau results with INERIS tests),

- the powder used is of higher reactivity (by comparison between aspirin or toner with charcoal in Lunn's experiments (K_{st} of 254, 236 and 144 bar.m/s respectively)),

- the duct diameter is wider (by comparison of INERIS tests between themselves).

Clearly, the trends are not respected and the proposed correlation in CEN standards should be used carefully. Note that in the NFPA 2007 standard, no minimal length of the duct is defined and it is advised to apply the procedure to account for the vent duct effect in so far as they are present.

7. Conclusion

New detailed experimental data on the incidence of vent ducts on the reduced explosion overpressures (P_{red}) for confined dust explosions was provided. The physical analysis reveals that the increase of P_{red} cannot be imparted to additional head losses into the pipe neither to extra flame acceleration inside the duct. It appears that the flame is passively pushed into the duct by the pressure in the vessel and that the combustion occurring during the flame transmission impedes the discharge of the vessel. The pipe acts more or less like a "plug".

Note however that this analysis is limited to rather short piece of pipe (less than 20 m) for which the installation of an exhaust pipe over a vent is of some practical significance. For much longer pipes the flame would acquire some autonomy and may further accelerate as demonstrated by previous experiments (Pineau, 1983). For gaseous explosions, the flame may significantly accelerate inside the pipe combustion and this may have a major incidence on P_{red} (Bouhard et al., 1990, Russo et al., 2007; Ponizy et al., 1999). Nevertheless, the latter findings were obtained at very small scale (laboratory) and the present authors did not manage to replicate them at the scale of Figure 3 with the same mixtures. Clearly, further research is required.

Keeping in mind those limitations and questions, a theoretical correlation linking P'_{red} (with the exhaust pipe) and P_{red} (without) was established and compared to the empirical correlations proposed in the official european standards and guidelines (VDI and EN14491). Not only none of these models describe accurately the effects of the vent ducts on the reduced pressure in the vessel but also there is clear evidence that in several configurations the P'_{red} measured experimentally is higher than the predicted one (see Figure 11 and Figure 12). Finally a minimal length l_{min} below which the duct is expected to have no effect on the pressure discharge is introduced in the CEN norms. In most of the cases, it seems that the model results are in good agreement with the experimental results. However, once more, in various situations, especially with larger ducts and bigger volumes, the model underestimates the effect of the duct. Thus one can conclude that despite providing comprehensive models for the vent-duct effect on the reduced pressure, in quite a wide range of situations the actual

CEN norms may lead to a significant underestimation of the pressure increase in the protected enclosure, leading to potentially unsafe situations.

References

Bartknecht, W. (1981), *Explosions: Course*, Prevention, Protection, Berlin: Springer-Verlag

Bonnet P. (2006), *Ω-19: Détermination des grandeurs caractéristiques du terme source necessaries à l'utilisation d'un modèle de dispersion atmosphérique des rejets accidentels*. N° INERIS-DRA-2005-P46055-C51076.

Bouhard F., Veyssière B., Leyer J. C. and Chaineaux J. (1990), Explosion in a vented vessel connected to a duct, *AIAA Prog. Astronaut. Aeronaut*. 134 (1990) 85–103

Kinney G.F.; Graham K.J. (1985), *Explosive Shocks in Air: Second Edition*, Springer-Verlag, New York, ISBN: 0-38-715147-8

Lewis B., Von Elbe G. (1987), *Combustion, flames and explosions of gases: 3rd edition*, Academic Press, London, ISBN 0-12-446751-2

Lunn G.A., Crowhurst D., Hey M. (1988), The effect of vent ducts on the reduced explosion pressures of vented dust explosions, *J. Loss Prev. Process Ind*., vol. 1

Lunn G.A., Nicol A.M., Collins P.D., Hubbard N.R. (1998), Effects of vent ducts on the reduced pressure from explosions in dust collectors, *J. Loss Prev. Process Ind*., vol 11

Pineau J.P. (1983), *Explosions de poussières dans des enceintes reliées à des canalisations*, article présenté au colloque "Sichere Handhabung brennbarer Stäube", Nüremberg, Oct. 1993

Ponizy, B. and Leyer, J.C., 1999a, Flame dynamics in a vented vessel connected to a duct: 1. Mechanism of vessel-duct interaction, *Combustion and Flame*, 116: 259–271.

Roux P. (2000), *Guide pour la conception et l'exploitation de silos de stockage de produits agroalimentaires vis à vis des risques d'explosion et d'incendie*, rapport INERIS, disponible sur site internet www.ineris.com

Roux P., Proust C. (2003), *Méthodes de protection contre les explosions : évents*, Rapport INERIS DRA-Pro-CPr-0225313

Russo P., and Di Benedetto A. (2007), The effects of duct on venting of explosions: critical review, *Process Safety and Environmental Protection*, 85, 9-22

Siwek R. (1989), *Dust Explosion Venting for Dusts pneumatically conveyed into Vessels*, Plant/Operation Progress, vol. 8

Siwek R., Van Wingerden K. (2006), Dust Explosion Venting: EN Standard 14491 vs.VDI-Guideline 3673, *Chemical Engineering Transactions,* Volume 9

Ural E. (2005), *"Dust Explosion Venting through Ducts."*, Proceedings of the 39th Annual Loss Prevention Symposium, American Institute of Chemical Engineers, Atlanta, GA, April 10–14.

AFNOR (1986), *Bâtiments agricoles et installations de stockage: Sécurité des silos*, NFU 54-540, ISSN 0335-3931.

NFPA 68, (2002), *Guide for Venting of Deflagration* National Fire Protection Association, Quincy, MA, USA.

NFPA 68, (2007), *Guide for Venting of Deflagration* National Fire Protection Association, Quincy, MA, USA

EN 14491 (2002), European Standard: *Dust explosion venting protective systems*. Ref. No.EN 14491:2002, European Committee for Standardization, Brussels, Belgium

EN 14491 (2012), European Standard: *Dust explosion venting protective systems*. Ref. No.EN 14491:2012, European Committee for Standardization, Brussels, Belgium

VDI 3673 (2002), *Pressure Release of Dust Explosions*, Guideline VDI 3673 1979, Beuth Verlag GmbH, 10772 Berlin, German

VDI 3673 (2002), *Pressure Release of Dust Explosions*, Guideline VDI 3673 Part 1:2002, Beuth Verlag GmbH, 10772 Berlin, Germany